Supplementary Materials

Fig. S1 Sequence alignment for DUSP3, DUSP5, and DUSP7. Figure S1(a) gives sequences of these DUSPs. Figure S1(b) gives the aligned 3D structures (shown in cartoon) from two different views. DUSP3, DUSP5, and DUSP7 are coloured orange, gray, and yellow, respectively. DUSP5 and DUSP7 are quite similar as typical DUSPs. The atypical DUSP3 has a longer loop near the catalytic centre's P-loop compared to DUSP5 and DUSP7. This structure difference is marked with the dashed red circle and the sequences are marked with the dashed red rectangle. The extra loop and alpha-helix at the N terminal of DUSP3 is marked with a blue circle. The corresponding sequence difference is marked with a blue rectangle.

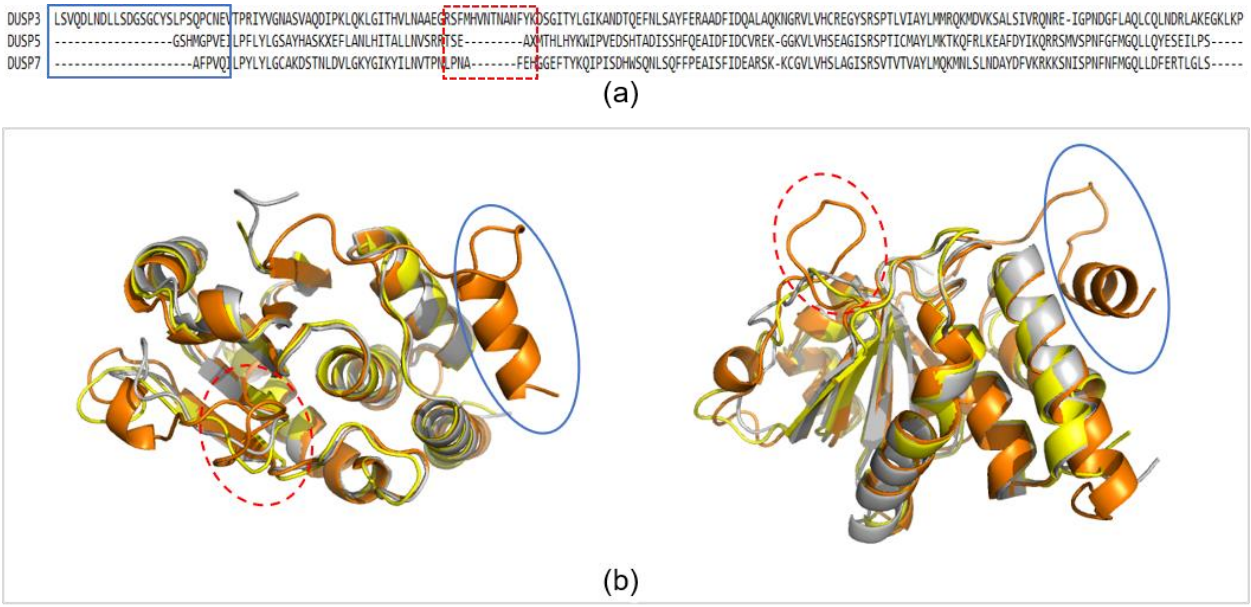

(a)

(b)

Fig. S2 Validation of the Glide docking protocol by docking the co-crystal ligand, STT, back to the binding pocket of DUSP3. The shown binding mode of redocked STT is the top 1 among redocking results with both the lowest docking energy and the lowest RMSD to STT's crystal structure. DUSP3 is represented as gray cartoon. STT in the crystal structure is shown as sticks and coloured by element with the magenta carbon. The docked-back STT is shown as sticks and coloured by element with green carbon.

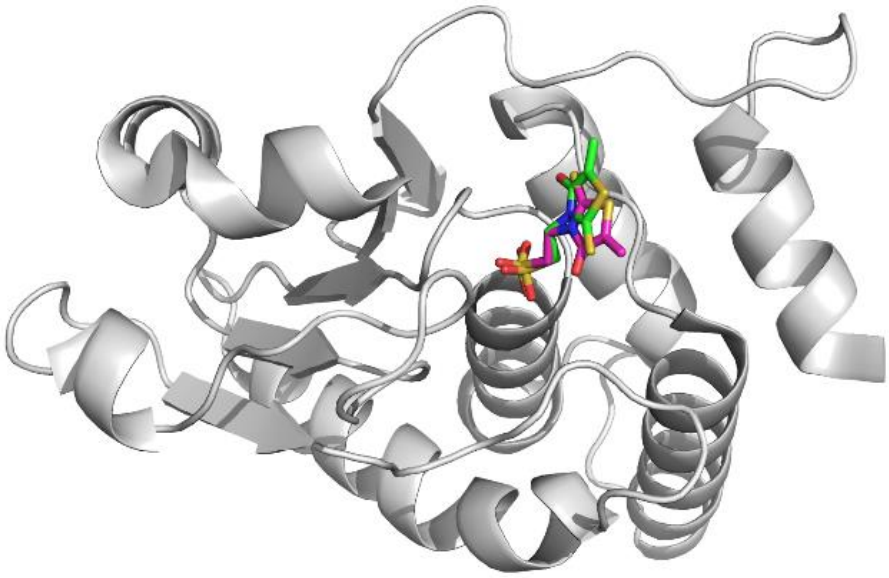

Fig. S3 Fluctuational patterns of Root-Mean-Square Deviations along the time course of MD simulations for DUSP3-ligand complexes. Black broken lines represent the RMSD of backbone heavy atoms of whole target proteins. Orange broken lines represent the RMSD of backbone heavy atoms of only secondary structures of target proteins. Blue broken lines represent the RMSD of least-square (LS) fitting ligands. Turquoise broken lines represent the RMSD of non-LS fitting ligands. non-LS fitting RMSDs were directly calculated for the ligand after the receptor was aligned to the reference structure.

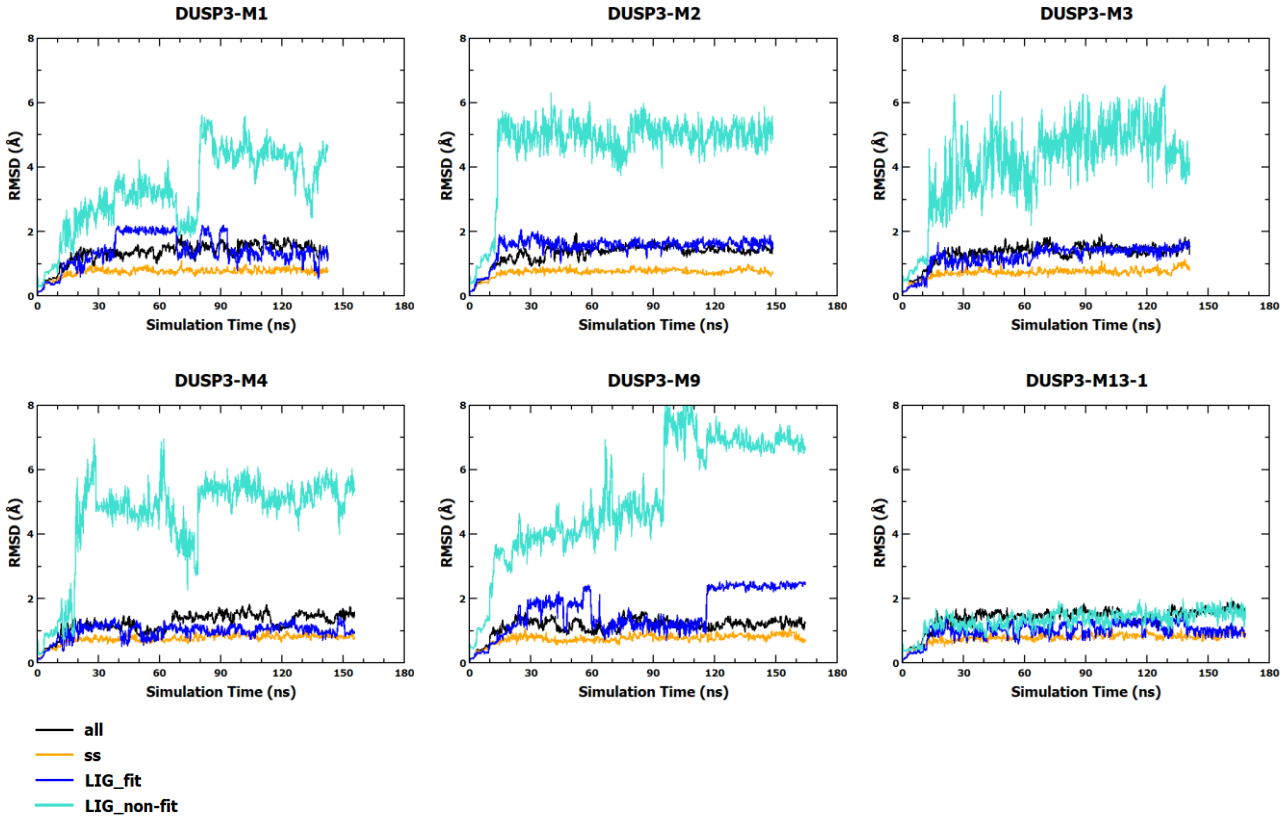

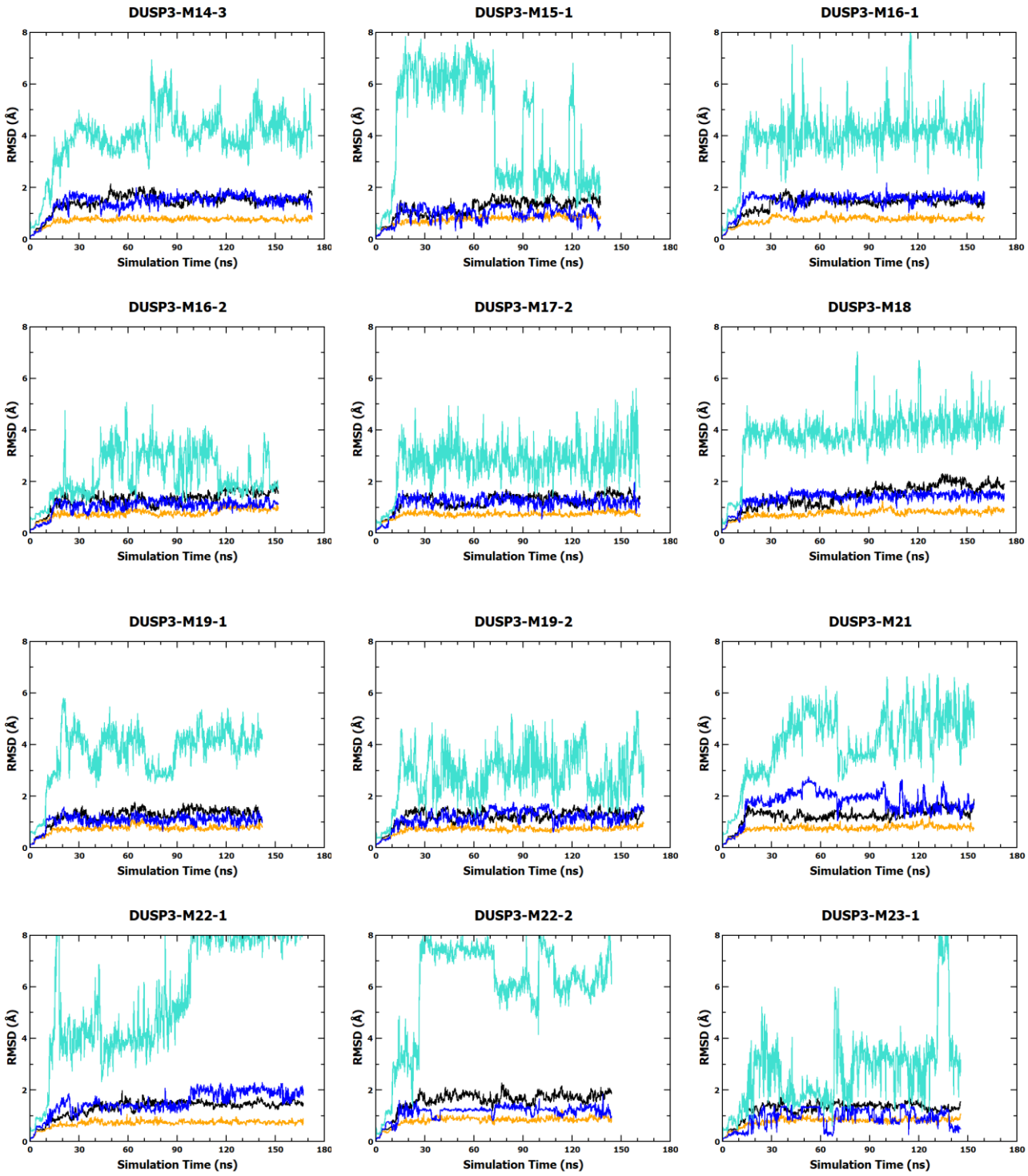
DUSP3-M14-3
DUSP3-M15-1
DUSP3-M16-1
DUSP3-M16-2
DUSP3-M17-2
DUSP3-M18
DUSP3-M19-1
DUSP3-M19-2
DUSP3-M21
DUSP3-M22-1
DUSP3-M22-2
DUSP3-M23-1
RMSD (Å)
Simulation Time (ns)

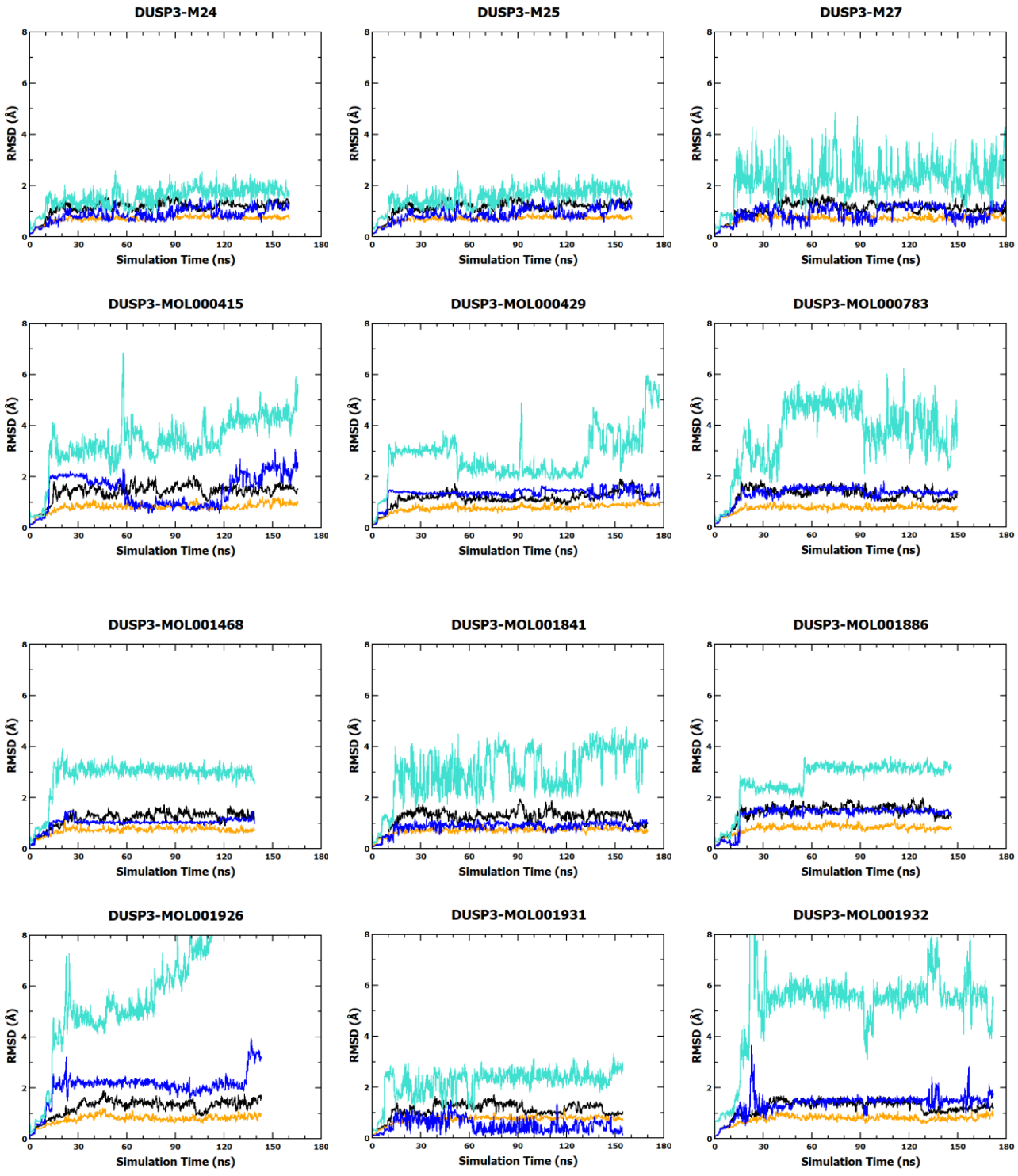
DUSP3-M24
DUSP3-M25
DUSP3-M27
DUSP3-MOL000415
DUSP3-MOL000429
DUSP3-MOL000783
DUSP3-MOL001468
DUSP3-MOL001841
DUSP3-MOL001886
DUSP3-MOL001926
DUSP3-MOL001931
DUSP3-MOL001932
RMSD (Å)
Simulation Time (ns)
0
30
60
90
120
150
180
2
4
6
8

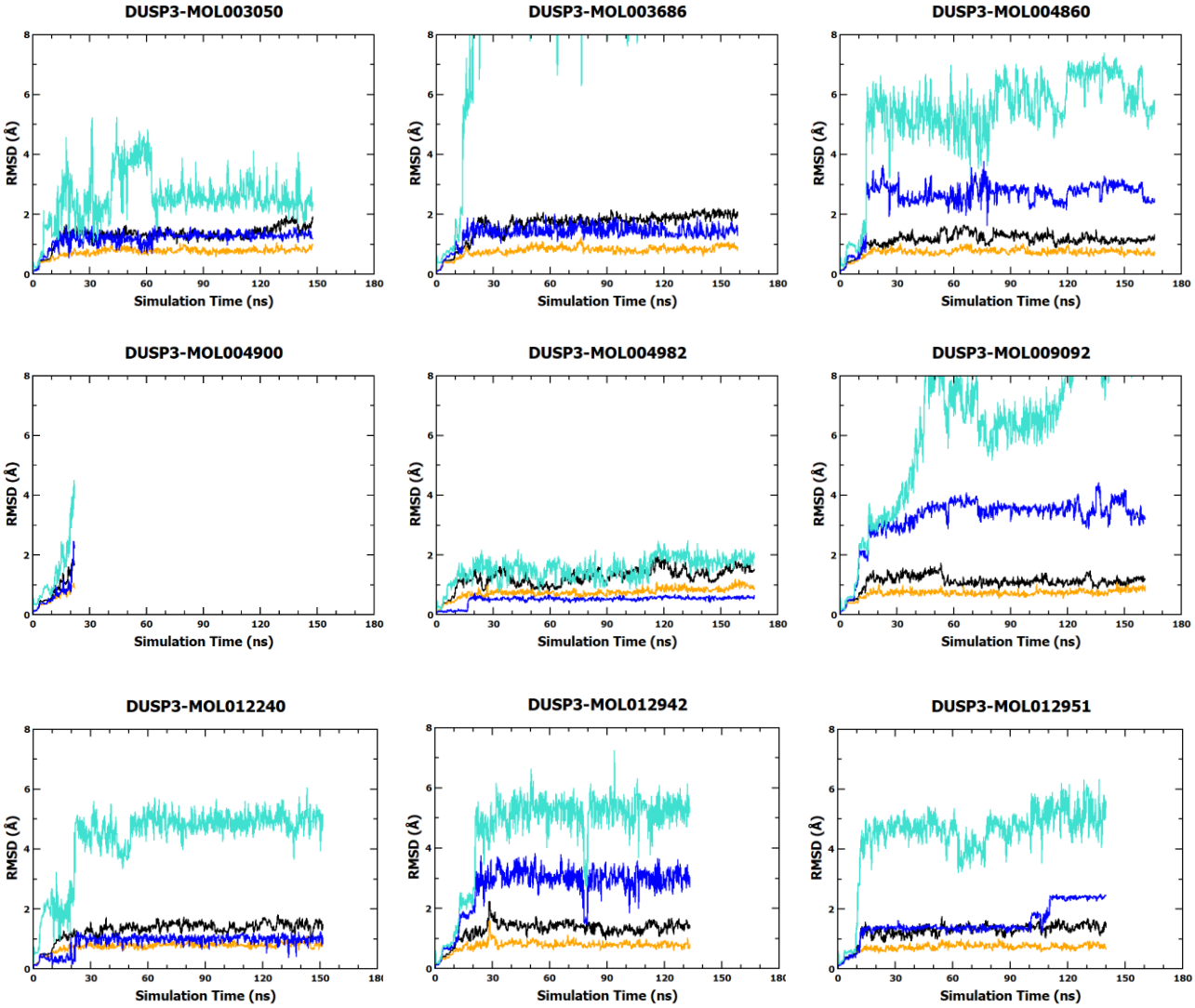
DUSP3-MOL003050
DUSP3-MOL003686
DUSP3-MOL004860
DUSP3-MOL004900
DUSP3-MOL004982
DUSP3-MOL009092
DUSP3-MOL012240
DUSP3-MOL012942
DUSP3-MOL012951
RMSD (Å)
Simulation Time (ns)

Table S1 Individual energy terms for DUSP3-ligand binding free energy calculations using the MM-PBSA method (energies in kcal/mol). Ligands with a positive value of $\Delta G_{MM/PBSA}$ are shown in red and considered as false positives of docking screening.

Ligand	ΔE_{vdW}^{gas}	ΔE_{eel}^{gas}	ΔG_{p}^{Sol}	ΔG_{np}^{Sol}	$T\Delta S$	$\Delta G_{MM/PBSA}$
M1	-37.14±0.06	-204.79±0.44	201.80±0.52	-3.25±0.01	-21.44±0.06	-21.93±0.11
M2	-33.32±0.28	-210.73±1.51	189.46±1.63	-2.94±0.01	-20.88±0.04	-36.65±0.33
M3	-32.86±0.10	-196.53±0.72	186.35±0.75	-2.88±0.01	-20.17±0.04	-25.74±0.10
M4	-29.05±0.18	15.56±0.44	10.77±0.48	-2.29±0.02	-17.08±0.01	12.08±0.44
M9	-34.97±0.28	17.19±0.46	12.70±0.24	-2.94±0.02	-18.37±0.06	10.34±0.28
M13-1	-42.92±0.11	-131.10±0.70	130.13±0.49	-3.07±0.00	-21.47±0.02	-25.50±0.27
M14-3	-32.91±0.14	-220.08±0.25	225.39±0.34	-2.49±0.01	-19.43±0.03	-10.66±0.15
M15-1	-33.80±0.04	-143.19±0.42	142.85±0.39	-2.19±0.01	-18.80±0.03	-17.52±0.03
M16-1	-35.39±0.25	-185.69±0.39	181.57±0.75	-3.00±0.02	-20.35±0.04	-22.16±0.18
M16-2	-29.54±0.34	-215.53±0.74	192.57±0.26	-2.77±0.01	-20.64±0.06	-34.62±0.31
M17-2	-28.53±0.17	-173.51±1.04	168.17±1.16	-2.66±0.01	-19.22±0.02	-17.31±0.12
M18	-40.32±0.13	-178.98±1.50	179.97±1.31	-3.07±0.00	-20.54±0.05	-21.85±0.38
M19-1	-38.92±0.16	-205.09±1.50	204.75±1.08	-3.10±0.02	-21.19±0.03	-21.16±0.47
M19-2	-33.96±0.27	-161.23±0.90	156.47±0.96	-2.67±0.01	-19.73±0.00	-21.66±0.11
M21	-38.75±0.23	-202.83±0.89	201.36±0.43	-3.27±0.02	-21.79±0.02	-21.69±0.37
M22-1	-34.62±0.40	-157.37±0.83	157.82±0.50	-2.48±0.01	-19.33±0.05	-17.32±0.53
M22-2	-32.09±0.55	-196.66±0.79	201.12±0.77	-2.77±0.01	-19.16±0.02	-11.24±0.26
M23-1	-32.49±0.11	-133.29±0.32	130.76±0.31	-2.00±0.01	-18.08±0.04	-18.94±0.20
M24	-38.25±0.26	-182.81±0.56	187.99±0.21	-3.42±0.00	-21.72±0.02	-14.78±0.20
M25	-35.28±0.06	-223.38±1.54	224.06±1.32	-3.39±0.01	-20.85±0.04	-17.14±0.40
M27	-31.93±0.11	-125.28±0.23	122.70±0.40	-2.07±0.01	-18.35±0.02	-18.22±0.34
MOL000415	-27.99±0.16	-38.53±0.13	53.77±0.45	-2.74±0.02	-18.03±0.05	2.54±0.37
MOL000429	-12.85±0.23	-103.72±0.28	115.33±0.27	-0.97±0.01	-15.68±0.03	13.47±0.23
MOL000783	-32.33±0.05	-219.76±1.47	228.59±1.06	-3.02±0.00	-19.52±0.01	-6.99±0.47
MOL001468	-10.54±0.14	-365.51±1.26	324.57±1.03	-0.80±0.00	-16.52±0.00	-35.76±0.20
MOL001841	-18.09±0.17	-156.91±0.49	139.78±0.31	-1.21±0.00	-16.26±0.01	-20.17±0.33
MOL001886	-11.43±0.16	-303.55±0.27	281.52±0.53	-0.88±0.00	-16.48±0.00	-17.87±0.37
MOL001926	-31.83±0.25	35.07±0.37	3.94±0.68	-2.94±0.02	-18.34±0.11	22.57±0.67
MOL001931	-15.19±0.06	-162.05±0.74	143.27±0.80	-0.82±0.00	-16.53±0.02	-18.25±0.20
MOL001932	-39.81±0.10	-21.07±0.51	42.81±0.57	-3.17±0.01	-19.81±0.07	-1.43±0.05

MOL003050	-19.44±0.21	-168.83±0.49	150.34±0.43	-1.42±0.01	-17.17±0.03	-22.18±0.16
MOL003686	-24.14±0.14	-41.26±0.52	47.35±0.38	-1.99±0.03	-16.71±0.07	-3.34±0.28
MOL004860	-46.46±0.08	-46.33±0.53	67.07±0.16	-4.21±0.02	-22.80±0.09	-7.13±0.25
MOL004900	0.00±0.00	0.00±0.00	0.00±0.00	0.00±0.00	0.00±0.00	0.00±0.00
MOL004982	-15.47±0.29	-167.69±0.28	154.75±0.07	-0.94±0.00	-16.05±0.01	-13.30±0.17
MOL009092	-41.18±0.08	-28.05±0.19	52.82±0.32	-3.57±0.01	-19.67±0.06	-0.31±0.18
MOL012240	-20.73±0.09	-14.85±0.64	30.85±0.37	-1.64±0.00	-15.68±0.03	9.32±0.29
MOL012942	-35.69±0.17	-17.29±0.28	51.82±0.16	-2.92±0.00	-17.83±0.05	13.74±0.11
MOL012951	-28.20±0.30	-175.48±0.64	165.28±0.45	-1.76±0.00	-18.56±0.02	-21.61±0.15

Fig. S4 RMSD ~ Simulation Time (RST) plots for DUSP5-ligand complexes. Legend description is the same with **Fig. S2**.

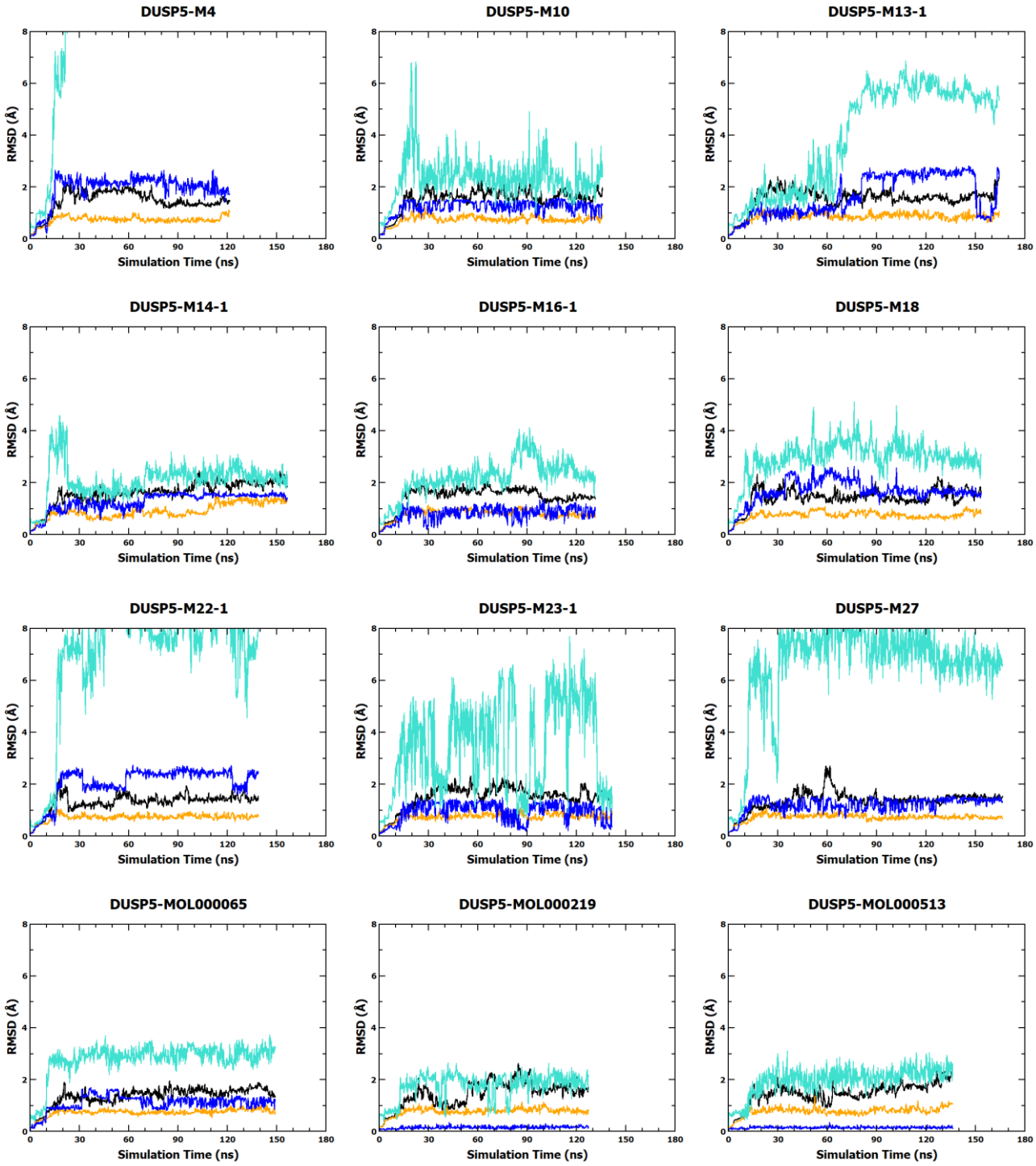

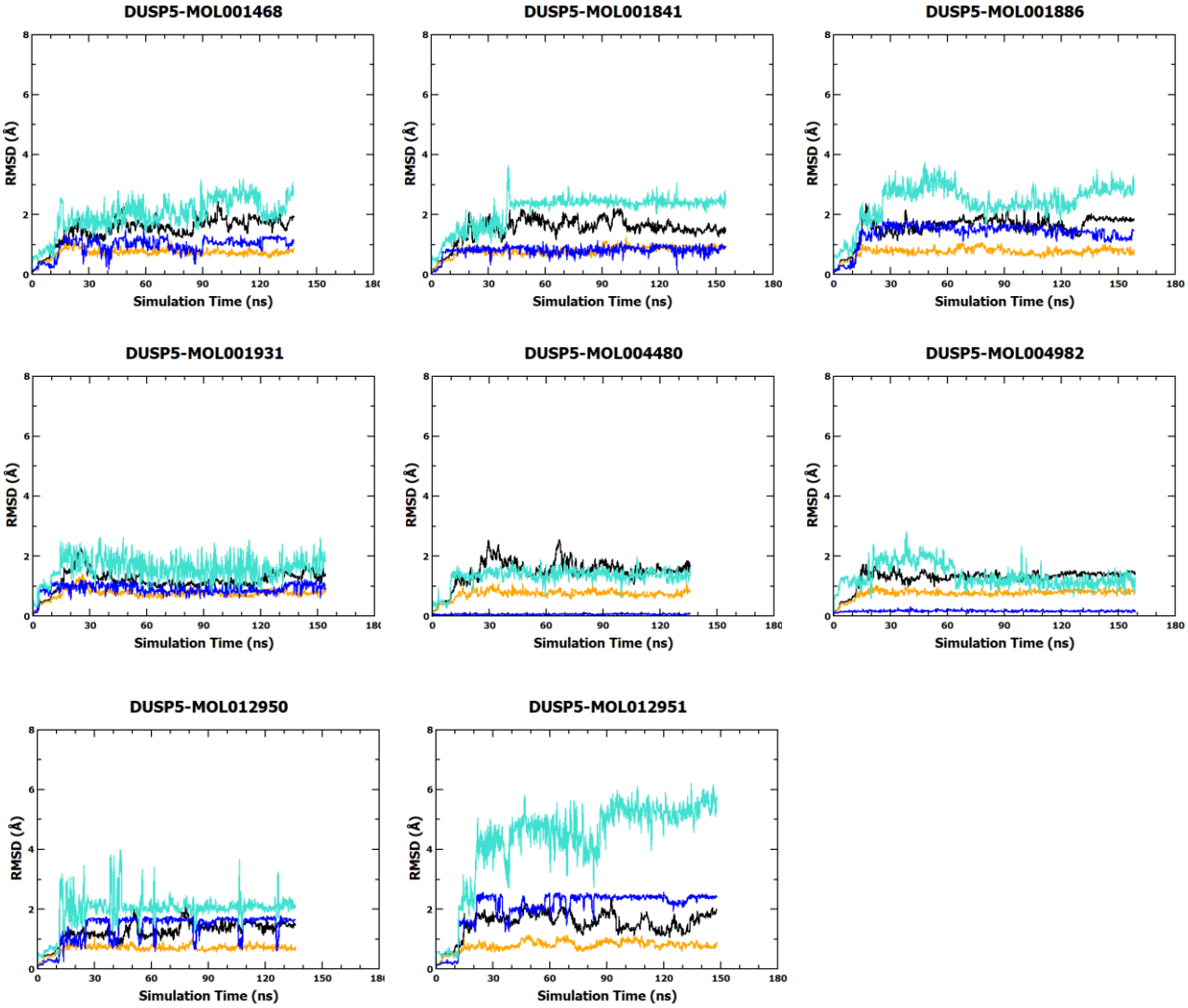
DUSP5-MOL001468
DUSP5-MOL001841
DUSP5-MOL001886
DUSP5-MOL001931
DUSP5-MOL004480
DUSP5-MOL004982
DUSP5-MOL012950
DUSP5-MOL012951
RMSD (Å)
Simulation Time (ns)

Table S2 Individual energy terms for DUSP5-ligand binding free energy calculations using the MM-PBSA method (energies in kcal/mol). Ligands with a positive value of $\Delta G_{MM/PBSA}$ are shown in red and considered as false positives of docking screening.

Ligand	ΔE_{vdW}^{gas}	ΔE_{eel}^{gas}	ΔG_{p}^{Sol}	ΔG_{np}^{Sol}	$T\Delta S$	$\Delta G_{MM/PBSA}$
M4	-22.55±0.06	-102.18±0.54	114.52±0.34	-1.87±0.01	-15.69±0.02	3.61±0.40
M10	-26.31±0.35	-141.49±0.41	135.52±0.31	-1.48±0.01	-16.99±0.02	-16.77±0.27
M13-1	-35.36±0.06	-213.23±1.10	210.57±1.12	-2.32±0.00	-19.29±0.03	-21.04±0.22
M14-1	-31.18±0.19	-293.41±1.09	280.59±1.37	-2.31±0.00	-19.66±0.02	-26.65±0.16
M16-1	-33.61±0.23	-152.90±0.38	155.01±0.29	-2.51±0.01	-19.43±0.04	-14.59±0.25
M18	-33.63±0.09	-243.16±3.08	240.33±2.91	-2.26±0.02	-19.35±0.04	-19.37±0.25
M22-1	-27.76±0.00	-184.87±0.53	178.28±0.60	-1.69±0.00	-18.06±0.06	-17.98±0.33
M23-1	-24.31±0.28	-122.63±0.82	115.41±0.61	-1.25±0.01	-16.43±0.05	-16.35±0.32
M27	-23.91±0.04	-127.68±0.63	120.39±0.77	-1.24±0.01	-16.49±0.02	-15.96±0.23
MOL000065	-9.88±0.20	-214.08±0.96	190.86±0.60	-0.77±0.00	-15.95±0.03	-17.92±0.27
MOL000219	-12.82±0.29	-159.96±0.32	141.84±0.51	-0.69±0.00	-14.99±0.01	-16.64±0.09
MOL000513	-12.92±0.37	-160.52±0.93	141.05±0.66	-0.82±0.00	-15.18±0.03	-18.03±0.23
MOL001468	-11.13±0.32	-218.97±1.93	201.49±1.49	-0.75±0.00	-15.61±0.01	-13.74±0.33
MOL001841	-16.92±0.23	-167.59±0.32	150.31±0.48	-0.91±0.00	-15.53±0.03	-19.58±0.22
MOL001886	-10.23±0.13	-290.37±0.57	267.28±0.66	-0.76±0.00	-15.73±0.01	-18.34±0.17
MOL001931	-11.55±0.04	-162.94±0.40	143.11±0.38	-0.67±0.00	-15.69±0.01	-16.36±0.26
MOL004480	-8.21±0.42	-190.79±0.46	160.96±0.56	-0.24±0.00	-14.04±0.01	-24.24±0.57
MOL004982	-14.38±0.11	-185.51±0.32	166.34±0.29	-0.82±0.00	-15.80±0.01	-18.57±0.13
MOL012950	-24.69±0.29	-177.21±0.07	162.16±0.42	-1.40±0.00	-17.62±0.03	-23.52±0.57
MOL012951	-24.78±0.07	-123.07±0.72	111.92±0.86	-1.29±0.01	-17.14±0.05	-20.08±0.13

Fig. S5 RMSD ~ Simulation Time (RST) plots for DUSP7-ligand complexes. Legend description is the same as **Fig. S2**.

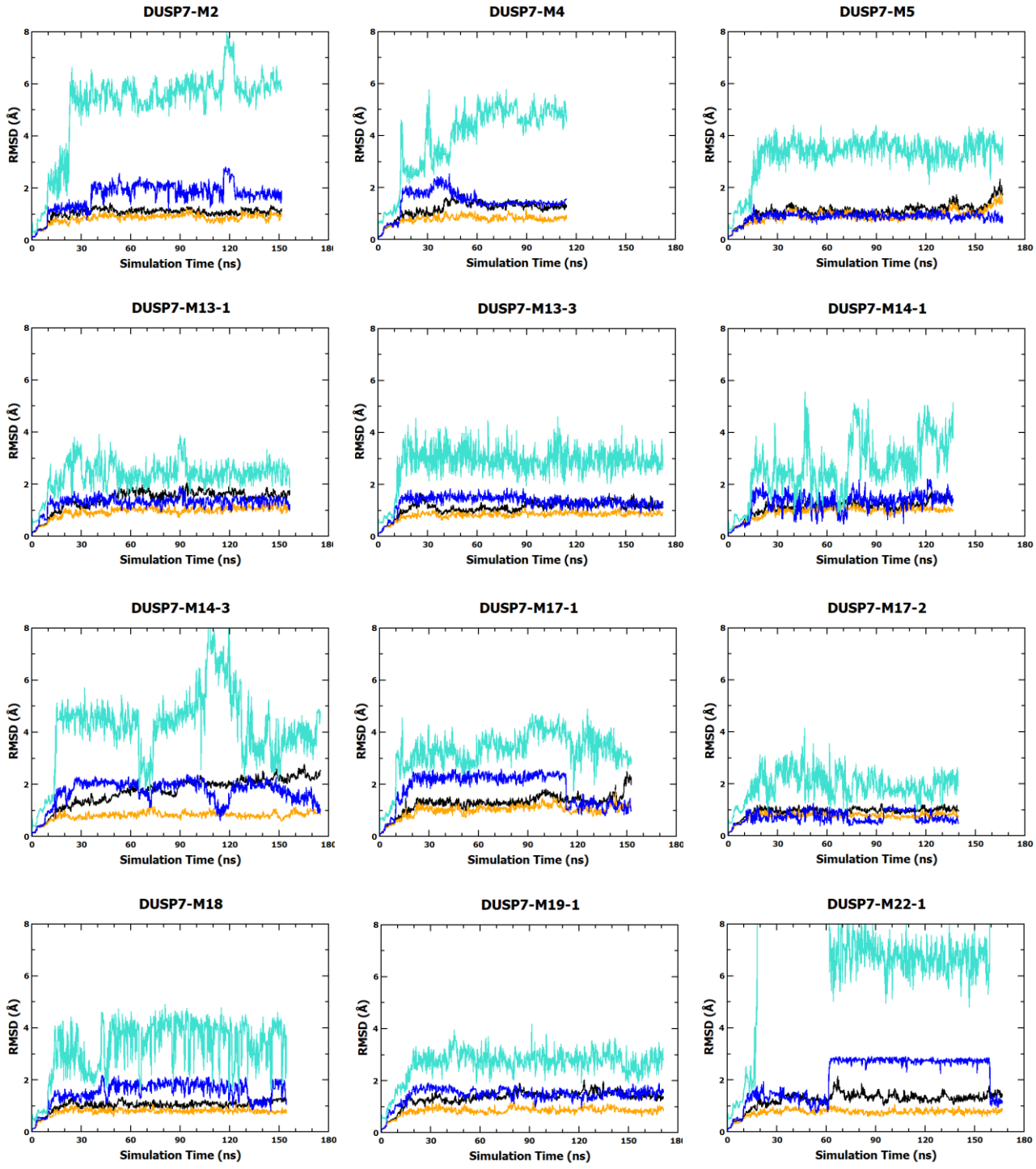

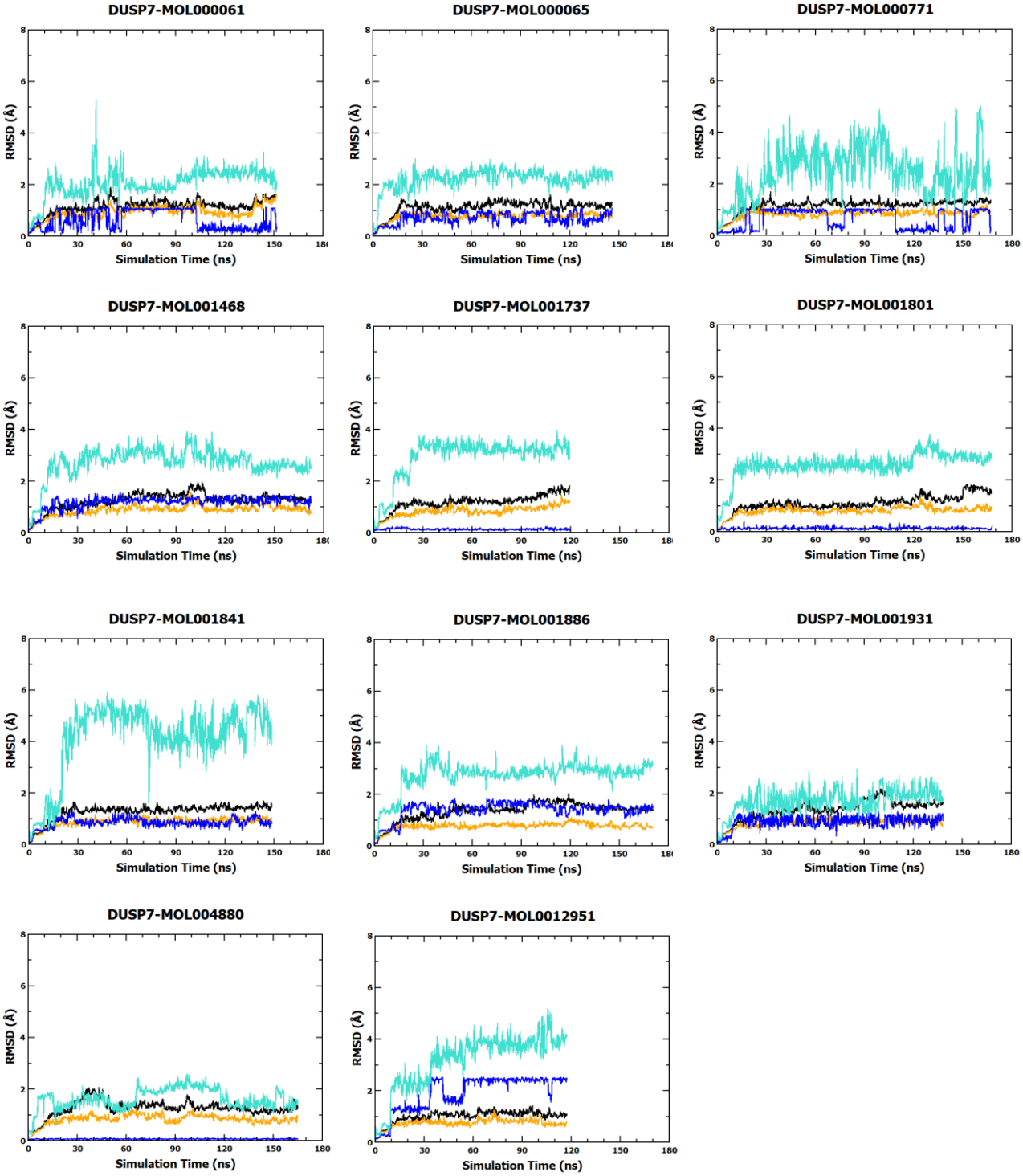
DUSP7-MOL000061
DUSP7-MOL000065
DUSP7-MOL000771
DUSP7-MOL001468
DUSP7-MOL001737
DUSP7-MOL001801
DUSP7-MOL001841
DUSP7-MOL001886
DUSP7-MOL001931
DUSP7-MOL004880
DUSP7-MOL0012951
RMSD (Å)
Simulation Time (ns)

Table S3. Individual energy terms for DUSP7-ligand binding free energy calculations using the MM-PBSA method (energies in kcal/mol). Ligands with a positive value of $\Delta G_{MM/PBSA}$ are shown in red and considered as false positives of docking screening.

Ligand	ΔE_{vdW}^{gas}	ΔE_{eel}^{gas}	ΔG_{p}^{Sol}	ΔG_{np}^{Sol}	$T\Delta S$	$\Delta G_{MM/PBSA}$
M2	-28.05±0.01	-334.82±0.74	311.93±0.46	-2.57±0.02	-20.91±0.02	-32.60±0.27
M4	-34.99±0.21	-229.22±2.09	223.36±1.39	-2.58±0.01	-20.10±0.05	-23.33±0.53
M5	-28.56±0.44	-243.84±0.83	226.98±0.84	-2.34±0.01	-20.00±0.04	-27.76±0.24
M13-1	-29.89±0.18	-345.54±0.56	321.20±0.57	-2.33±0.02	-20.10±0.05	-36.46±0.01
M13-3	-21.43±0.20	-335.62±0.36	311.08±0.68	-1.62±0.00	-18.41±0.02	-29.18±0.21
M14-1	-33.11±0.11	-251.07±1.06	256.44±1.43	-2.18±0.01	-18.56±0.02	-11.36±0.37
M14-3	-27.75±0.06	-335.77±0.48	321.36±0.47	-1.88±0.01	-18.76±0.20	-25.27±0.30
M17-1	-29.85±0.13	-171.55±0.17	193.87±0.01	-2.38±0.01	-18.09±0.00	8.19±0.32
M17-2	-29.09±0.16	-212.70±0.87	204.59±0.71	-2.24±0.01	-18.70±0.02	-20.74±0.35
M18	-33.30±0.56	-340.89±0.60	323.14±0.70	-2.44±0.03	-20.73±0.09	-32.76±0.49
M19-1	-33.38±0.26	-330.13±0.48	326.51±0.16	-2.69±0.01	-19.66±0.06	-20.04±0.13
M22-1	-25.91±0.32	-211.58±1.35	203.09±1.13	-2.09±0.03	-18.27±0.10	-18.22±0.30
MOL000061	-11.08±0.14	-69.25±0.29	72.11±0.54	-0.71±0.00	-14.84±0.01	5.91±0.31
MOL000065	-9.96±0.20	-278.89±0.89	252.88±0.72	-0.81±0.00	-16.03±0.03	-20.76±0.33
MOL000771	-12.49±0.33	-230.19±0.68	209.35±0.12	-0.92±0.01	-14.86±0.03	-19.39±0.33
MOL001468	-8.98±0.22	-397.56±1.04	370.55±0.69	-0.73±0.00	-15.85±0.02	-20.86±0.22
MOL001737	-15.32±0.19	-218.12±0.20	201.21±0.19	-1.01±0.01	-15.24±0.02	-18.00±0.17
MOL001801	-14.80±0.04	-198.65±0.40	184.16±0.10	-0.82±0.00	-15.26±0.01	-14.84±0.32
MOL001841	-12.98±0.06	-230.24±0.85	211.94±0.45	-1.13±0.00	-15.43±0.03	-16.98±0.43
MOL001886	-10.45±0.29	-376.06±1.16	354.42±1.13	-0.81±0.00	-15.99±0.03	-16.92±0.22
MOL001931	-11.80±0.02	-209.91±0.28	189.50±0.35	-0.79±0.00	-15.68±0.02	-17.32±0.11
MOL004480	-5.18±0.32	-238.60±0.46	209.04±0.17	-0.25±0.00	-14.10±0.01	-20.89±0.12
MOL012951	-26.83±0.17	-185.28±0.63	175.53±0.57	-1.70±0.02	-17.81±0.03	-20.47±0.15

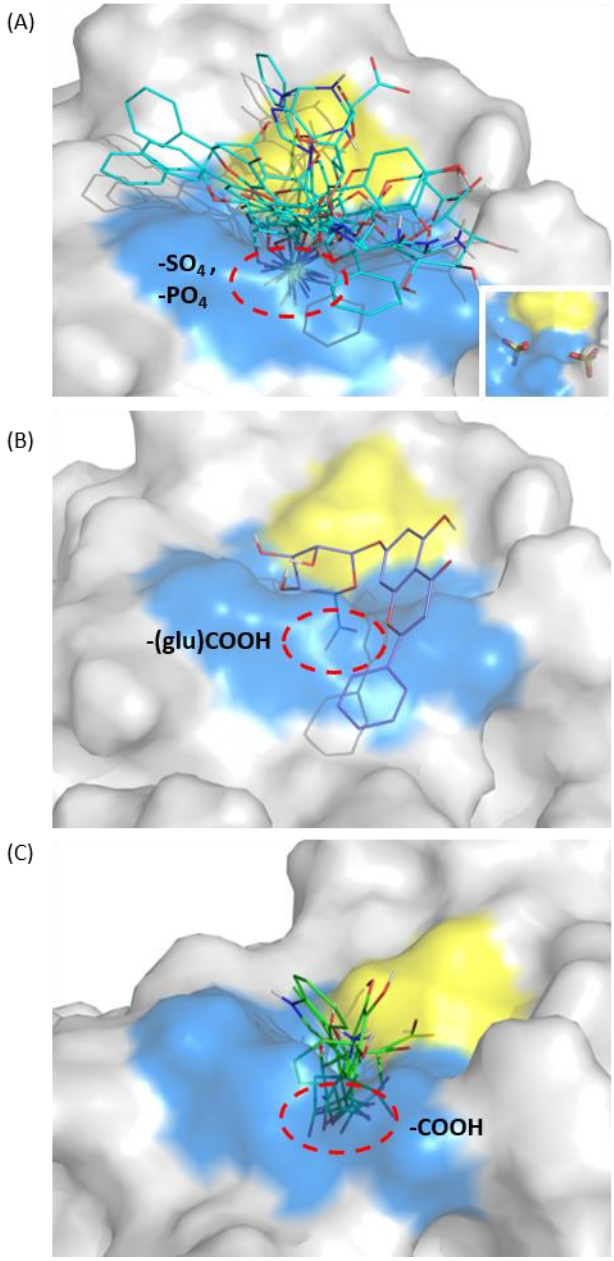

Fig. S6 Common substituent groups of advantageous DUSP5 ligands from YIY-906. The protein DUSP3 is represented as surface with the P-loop coloured blue and the D-loops coloured yellow. Ligand binding modes are demonstrated using the representative conformations of MD simulations. Specifically, sulfate ions in the crystal structure of DUSP5 are shown in the right corner of Panel (A). Common substituent groups (-SO_4, -PO_4, and -COOH) are marked with dashed red circles. (A) the binding of phosphate groups and sulfate groups in the protein's active pocket; (B) the binding of carboxyl groups of glucuronic acids on YIV-906 metabolites in the protein's active site; (C) the binding of carboxyl groups of original YIV-906 chemicals in the protein's active site. The perspective of each ligand-protein complex was slightly adjusted to achieve a clearer view. The surface transparency was set to 60% to show the parts of ligands which stick into the pocket but are concealed by nearby surface.

Fig. S7 Common substituent groups of advantageous DUSP7 ligands from YIY-906. Specifically, the phosphate ion in the crystal structure of DUSP7 are shown in the right corner of Panel (A). Other captions are the same as that of **Fig. S6**.

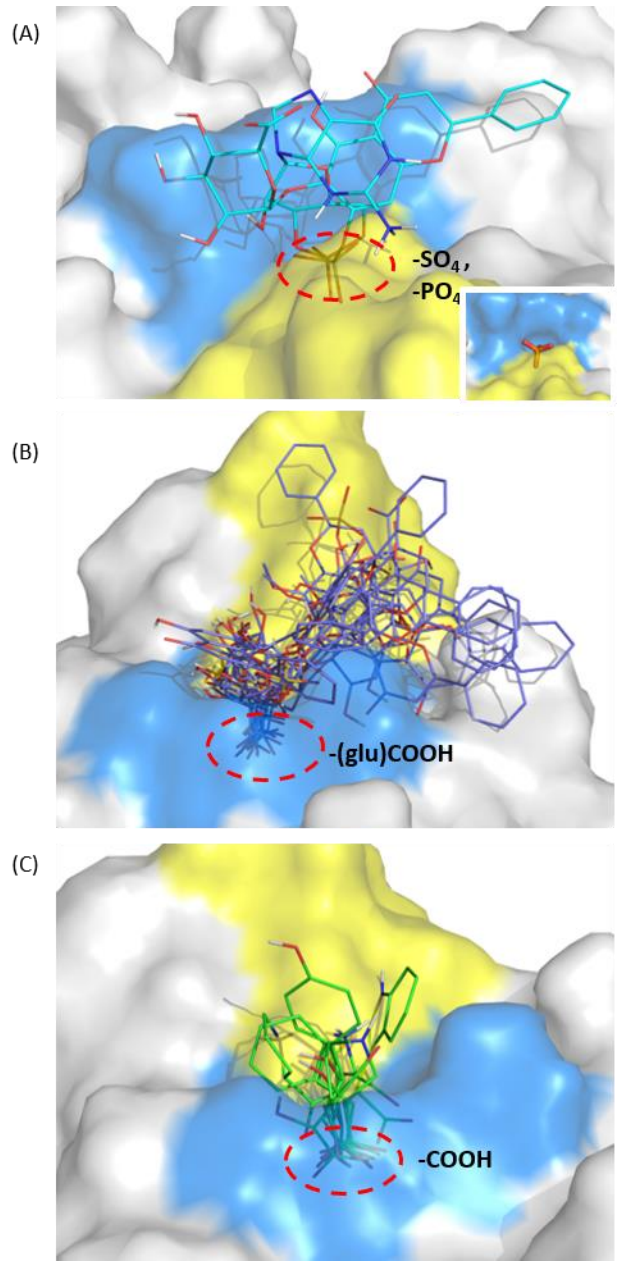

Fig. S8 Comparison of the binding modes predicted by docking and MD simulations for DUSP3. For each DUSP3-ligand complex, the representative MD snapshot, which has the smallest RMSD to the average structure of collected MD frames, was selected and aligned to the crystal structure. The receptor is represented using golden and marine blue cartoons for the docking and MD modes, respectively. The common ligands are shown as sticks using the same colour scheme.

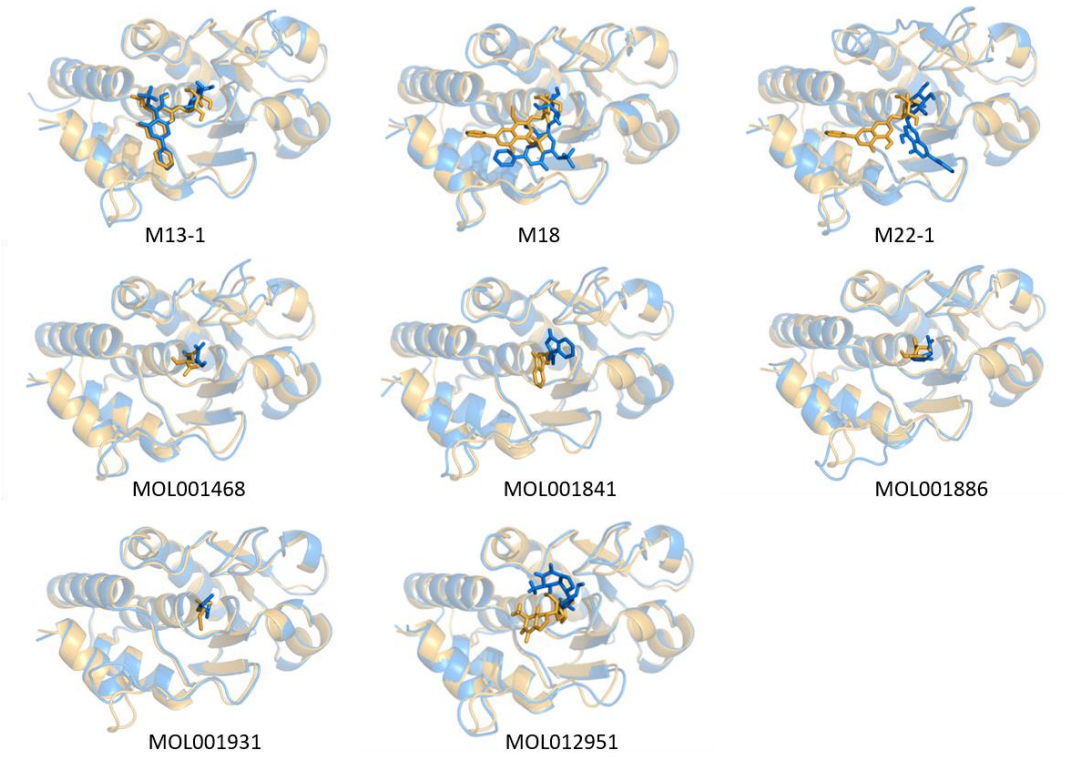

Fig. S9 Comparison of the binding modes predicted by docking and MD simulations for DUSP5. For each DUSP5-ligand complex, the representative MD snapshot, which has the smallest RMSD to the average structure of collected MD frames, was selected and aligned to the crystal structure. Other captions are the same as that of **Fig. S8**.

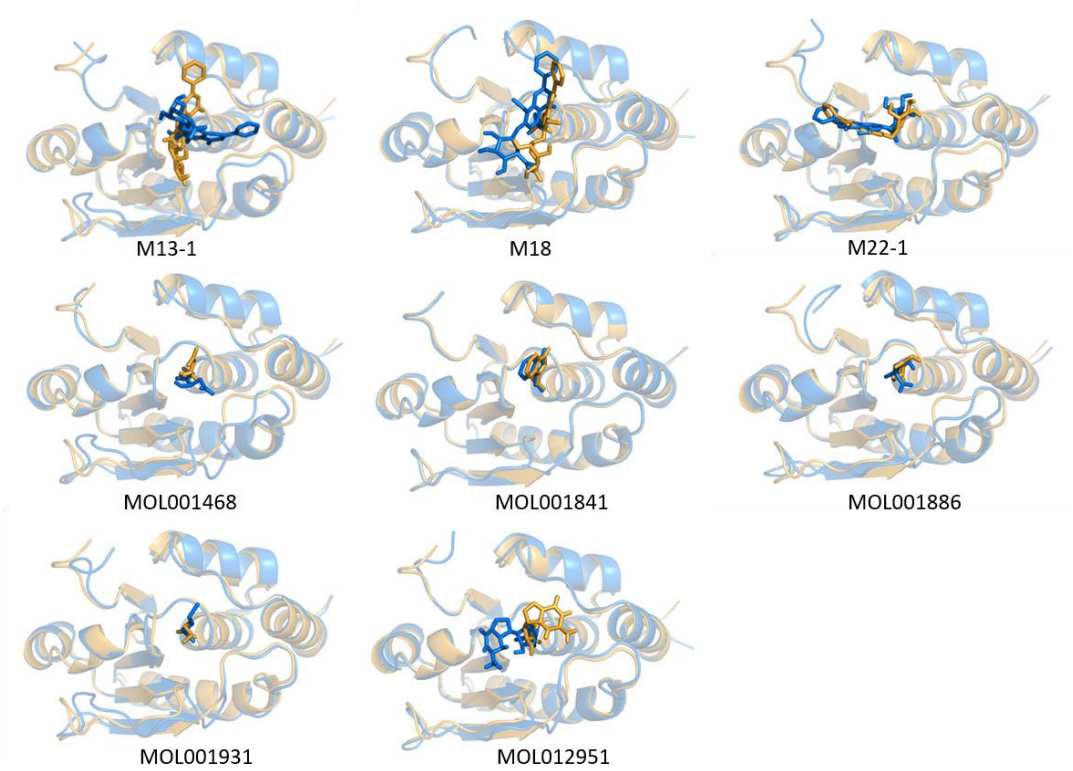

Fig. S10 Comparison of the binding modes predicted by docking and MD simulations for DUSP7. For each DUSP7-ligand complex, the representative MD snapshot, which has the smallest RMSD to the average structure of collected MD frames, was selected and aligned to the crystal structure. Other captions are the same as that of **Fig. S8**.

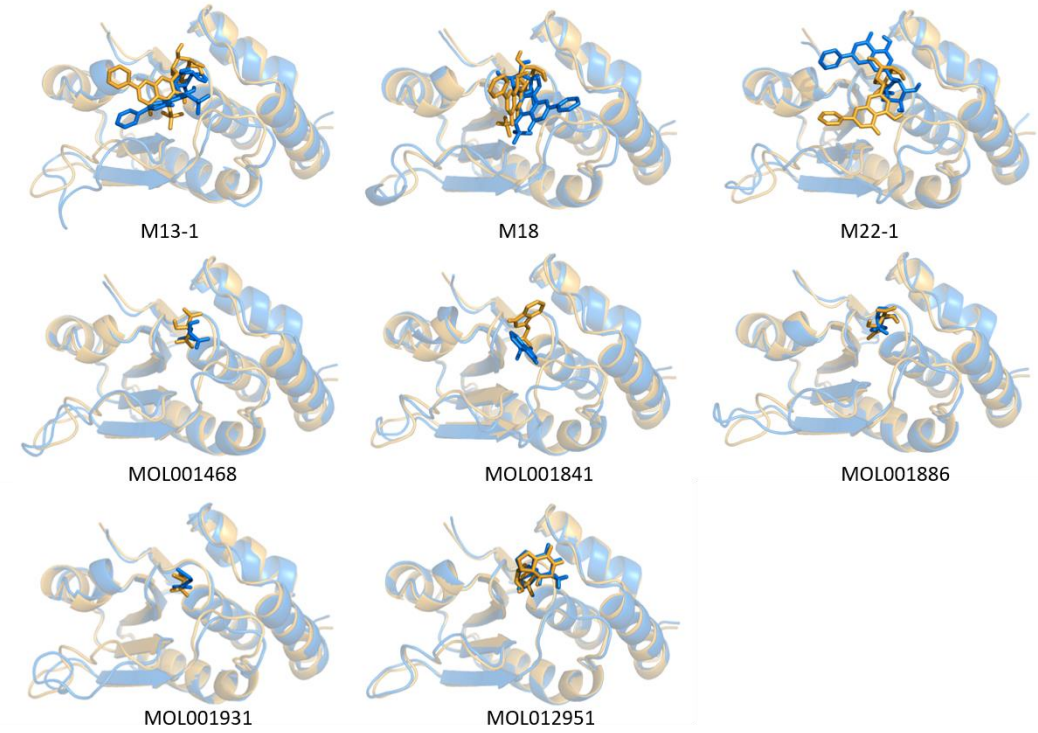

Fig. S11 Binding modes of the M13-1 metabolite with DUSP3, DUSP5, and DUSP7. DUSPs are shown as cartoon and M13-1 is shown in lines. The dominant tones of DUSP3-M13-1 complex, DUSP5-M13-1 complex, and DUSP7-M13-1 complex are dark blue, purple, and green, respectively. The carbon and sulfate elements on the ligand functional groups are labeled. The transparency of DUSPs was set to 60%.

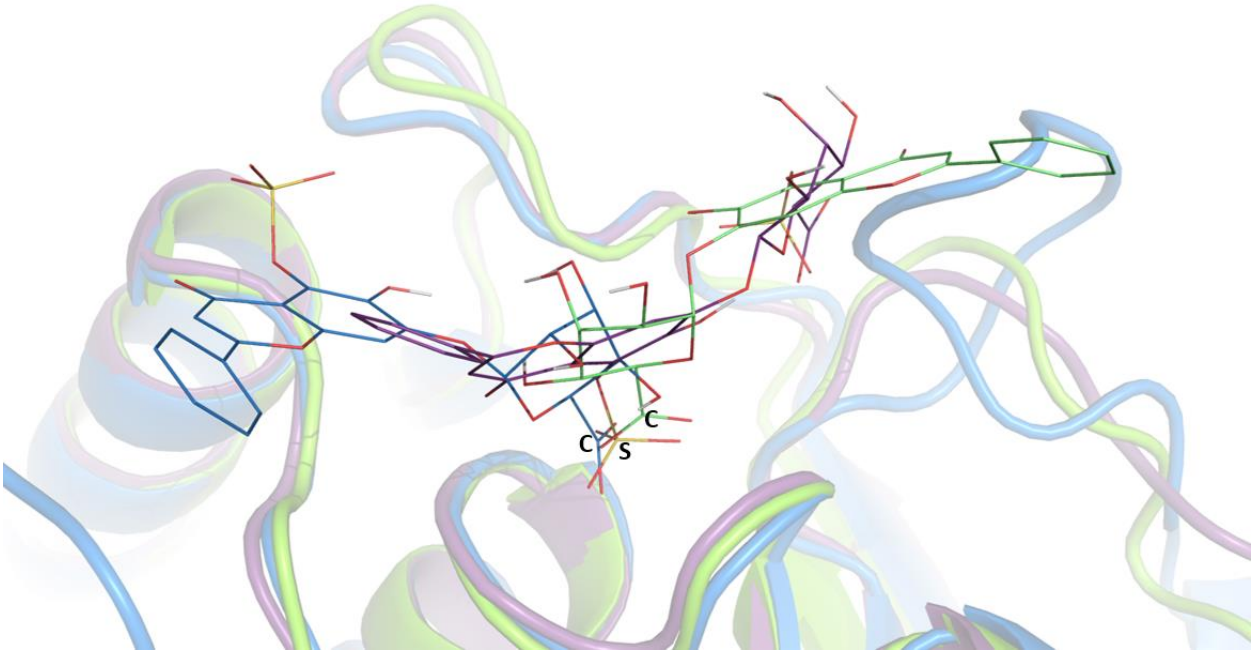

Table S4. MM/PBSA-predicted electrostatic energy ($\Delta E_{ele} + \Delta G_p^{sol}$), $\Delta G_{MM/PBSA}$ and calibrated $\Delta G_{MM/PBSA}$ for randomly selected bioassay compounds. Compounds with values of $\Delta G_{MM/PBSA}$ shown in green are MM/PBSA identified as good bioassay inhibitors. Compounds with values of $\Delta G_{MM/PBSA}$ shown in red are MM/PBSA identified as weak bioassay inhibitors.

BIOASSAY COMPOUND	$(\Delta E_{ele} + \Delta G_p^{sol})$	$\Delta G_{MM/PBSA}$	*Experimental* ΔG	*Calibrated* $\Delta G_{MM/PBSA}$
CHEMBL386313	-16.61	-21.21	-7.77	-7.29
CHEMBL1412062	-9.97	-19.12	-7.75	-7.04
CHEMBL185003	-34.42	-35.72	-7.55	-7.95
CHEMBL565364	-9.41	-23.50	-7.51	-7.02
CHEMBL585291	-12.26	-22.63	-7.44	-7.13
CHEMBL1333409	13.64	-1.28	-7.38	-6.16
CHEMBL1602125	-9.53	-21.9	-6.71	-7.02
CHEMBL212723	3.90	9.04	-6.63	-6.52
CHEMBL565581	-9.12	-18.38	-6.63	-7.01
CHEMBL1363824	-3.93	-14.41	-6.40	-6.81
CHEMBL567686	12.16	1.45	-6.30	-6.21
CHEMBL1612148	19.96	6.07	-5.71	-5.92
CHEMBL1414573	14.17	5.26	-5.57	-6.14
CHEMBL585314	4.10	-13.79	-5.39	-6.51